Polar magnetic metallic state in few-layer $BiFeO_3$

Marco Campetella[1,2,*] and Matteo Calandra[3,4,2,†]
[1]*Consiglio Nazionale Delle Ricerche (CNR) SPIN, I-00133 Rome, Italy*
[2]*Sorbonne Université, CNRS, Institut des Nanosciences de Paris, UMR7588, F-75252 Paris, France*
[3]*Department of Physics, University of Trento, Via Sommarive 14, I-38123 Povo, Italy*
[4]*Graphene Labs, Fondazione Istituto Italiano di Tecnologia, Via Morego, I-16163 Genova, Italy*

(Received 2 July 2021; accepted 28 October 2021; published 23 November 2021)

Recently, few-layer suspended stoichiometric $BiFeO_3$ flakes were synthesized and found to display large tetragonality and giant dipole moments per unit surface. Little is known, however, about the ground state properties of this compound in the two-dimensional (2D) limit. By performing first-principles electronic structure calculations, we determine the ground state structural, magnetic, and electronic properties of suspended stoichiometric $BiFeO_3$ flakes with number of layers (n) ranging from 1 to 4. We show that, even if the orthorhombic flakes with G-type antiferromagnetic order are the most stable ones for $n \leqslant 4$, the metastable cubic $BiFeO_3$ multilayers have physical properties in excellent agreement with experimental data, including enhanced tetragonality and large dipole moments per unit surface in the 2D limit. In these cubic multilayers, the broken inversion symmetry, determined by the different top and bottom terminations, results in a strong Fe offset along the z direction coexisting with metallicity. Our work shows that the cubic phase, nonmagnetic and stable only above 927 K in bulk and in thin films, is a "polar" magnetic metal and a type I "multiferroic" in the 2D limit at room temperature.

DOI: 10.1103/PhysRevB.104.174111

I. INTRODUCTION

Recently, it has been shown that few-atoms-thick two-dimensional freestanding stoichiometric $BiFeO_3$ and $SrTiO_3$ perovskites can be isolated down to the monolayer limit [1] by using experimental exfoliation techniques based on water-soluble $Sr_3Al_2O_6$ as sacrificial buffer layer [1–3]. Furthermore, freestanding single-crystalline multiferroic $BiFeO_3$ membranes for application in flexible electronics have been developed [4]. These findings open new perspectives in the exploration of correlated phases such as magnetism, high-T_c superconductivity [5], ferroelectricity [6], and multiferroicity [7] in low dimensional oxydes.

Little is known, however, about the ground state properties of freestanding few-layer $BiFeO_3$. Experiments show that, as the thickness of the thin film decreases, the in-plane lattice parameter (a) shrinks and the out-of-plane Bi-Bi distance (c) expands, resulting in an abnormal c/a ratio (≈ 1.22). A giant dipole moment per unit surface (140 $\mu C/cm^2$) along the out-of-plane direction is observed via piezoresponse force microscopy. Thus, surprisingly, $BiFeO_3$ displays giant tetragonality ($c/a > 1$) and large dipole moments per unit surface in the 2D limit, at odd with what happens in the case of thicker films supported on $SrTiO_3$ (showing no tetragonality) and with the bulk case showing the occurrence of a tetragonal structure only at very high temperatures, above 977°C (see Fig. 1). The theoretical calculations in Ref. [1] claimed that the most stable stoichiometric $BiFeO_3$ multilayer has a tetragonal symmetry (space group 99) with G-type spin polarization [8]. Thus, the ground state of few-layer $BiFeO_3$ seems to be hard to infer from the data available on the bulk or on thicker films. Furthermore, the ground state magnetic properties for these $BiFeO_3$ two-dimensional (2D) samples are unknown, no transport data are available, and calculations of the electronic structure and "polar" properties are missing in the literature.

In this work we perform an extensive study of all possible polytypes and magnetic orders of stoichiometric $BiFeO_3$ n-layers with $n \leqslant 4$. We show that in the absence of strain, the most stable polytype is the orthorhombic one with G-type antiferromagnetic order. This system displays a transition from an indirect to a direct gap insulating state by reducing thickness. Most importantly, we demonstrate that the metastable cubic ferromagnetic multilayers have structural parameters, enhanced tetragonality, and large dipole moments per unit surface, in excellent agreement with the experimentally synthesized suspended stoichiometric $BiFeO_3$ multilayers in Ref. [1] but in disagreement with the theoretical claim in Ref. [1]. Finally, we show that these flakes are metals hosting a large dipole moment per unit surface and are type I multiferroic in the 2D limit at room temperature (following the classification of Refs. [9,10]).

Bulk $BiFeO_3$ is a multiferroic [11–17] with coexistence of both antiferromagnetism (Néel temperature $T_N = 377\,^\circ C$) [18,19] and ferroelectricity (ferroelectric critical temperature, $T_F = 810$–$830\,^\circ C$) [20,21]. As ferroelectricity sets in above the Néel temperature, it is usually considered a type I multiferroic [9,10]. The $BiFeO_3$ bulk phase diagram reveals the presence of four different phases, as shown in the top panel of Fig. 1. At room temperature the most stable polytype has rhombohedral (R) symmetry and crystallizes in the $R3c$ space

*marco.campetella@spin.cnr.it
†m.calandrabuonaura@unitn.it

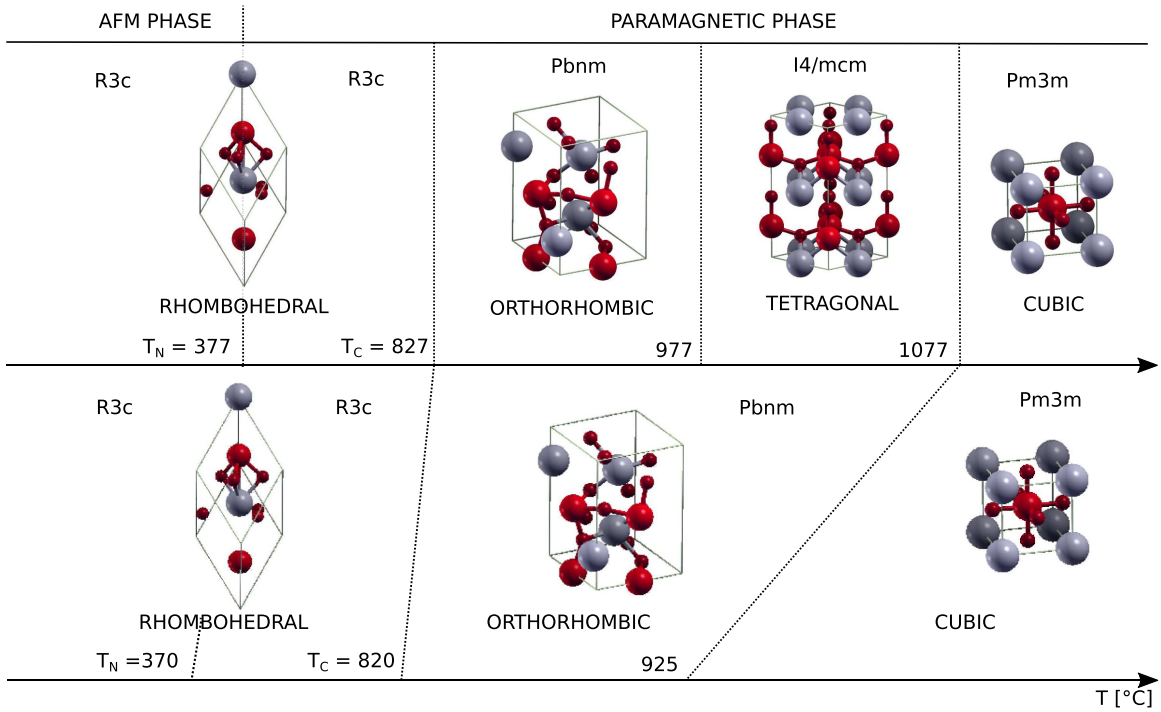

FIG. 1. Top panel: Finite temperature phase diagram of bulk $BiFeO_3$. The space groups of the different bulk phases as a function of increasing temperature are *R*3*c*, *Pbnm*, *I*4/*mcm*, and *Pm*3*m*. The Bi atoms are reported in gray, the O atoms in dark red, the Fe atoms in red. The Néel temperature and Curie temperature are also reported (from Ref. [25]). Bottom panel: The same but for $BiFeO_3$ grown by pulsed laser deposition on $SrTiO_3$(001) (from Ref. [20]).

group. At about 827 °C (well above T_N) a phase transition occurs to an orthorhombic (O) structure with space group *Pbnm* and no magnetic order. A second phase transition to a tetragonal (T) phase with space group *I*4/*mcm* follows at 977 °C. Finally a metallic cubic (C) phase (space group *Pm*3*m*) is the most stable one in the 1077–1127 °C temperature range [20,22–25]. All phases, except the cubic one, are insulating.

The phase diagram of thin films (thickness of 70–200 Å) grown on $SrTiO_3$ has been very well characterized both experimentally and theoretically and is shown in the bottom panel of Fig. 1. It is similar to the bulk case, except for the fact that the tetragonal phase has disappeared and the cubic metallic phase is stable at much lower temperatures. The thin-film phase diagram can be further modified by applying epitaxial strain via substrate. Epitaxial strain can stabilize $BiFeO_3$ into two main crystal structures, the so-called T and R phases, while the cubic metallic remains the most stable one at very high temperatures.

The T phase refers to a parent tetragonal phase with *P*4*mm* symmetry that has a c axis lattice parameter of ∼4.65 Å (tetragonality c/a ratio ∼ 1.2) and encompasses small monoclinic distortions from this tetragonal symmetry. The R phase refers to a distorted form of the *R*3*c* phase of the bulk, associated with its pseudocubic (PC) unit cell (a = 3.96 Å, α = 89.4°); see Fig. 2 that has a c axis lattice parameter of ∼ 4.01 (no tetragonality, i.e., c/a ratio ∼ 1.0) [26,27]. Hence, this phase is obtained by a cut of bulk rhombohedral structure perpendicular to $[012]_{\text{hex}}$ that corresponds to the $[010]_{pc}$ direction of the new pseudocubic phase [28,29]. To better explain the relation between the hexagonal and the pseudocubic phases Fig. S5 has been added in the Supplemental Material (SM) [30] We will see now that the ground state of few-layer $BiFeO_3$ can hardly be inferred from the knowledge of Fig. 1.

II. COMPUTATIONAL DETAILS

We perform density functional theory calculations with the gradient corrected Perdew-Burke-Ernzerhof (PBE) [31] functional by using the QUANTUM ESPRESSO (QE) package [32,33]. Hybrid functional electronic structure calculations (PBE0 functional [34]) are performed using the CRYSTAL code [35]. We have verified that the two codes lead to perfectly consistent results. In the case of multilayers, we use a truncated Coulomb interaction in the direction perpendicular to the layers, following the work of [36] or, for the CRYSTAL

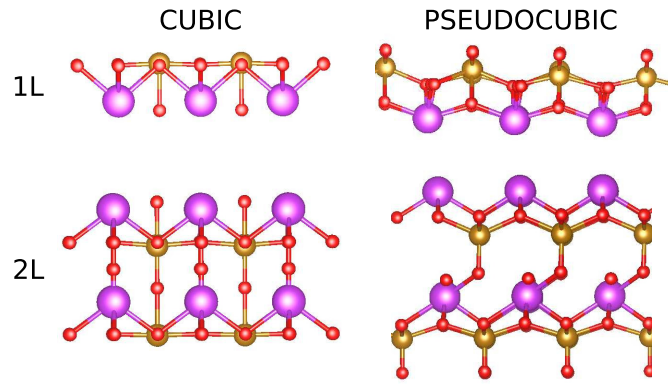

FIG. 2. Comparison between cubic and pseudocubic multilayer systems (1L and 2L).

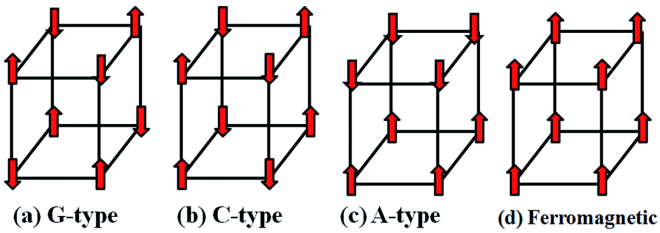

FIG. 3. Magnetic states considered in the calculation. A-type AFM has ferromagnetic couplings within each Fe layer and antiferromagnetic interlayer couplings, C-type AFM has antiferromagnetic couplings within each iron layer and ferromagnetic interlayer couplings, and finally G-type AFM has both intralayer and interlayer antiferromagnetic couplings.

code, we use open boundary conditions perpendicular to the flakes. More technical details are given in the *Computational details* section of SM [30] (see, also, Refs. [5–9] therein).

III. RESULTS

We first validate the reliability of our geometrical optimization on the bulk phase of $BiFeO_3$. We consider the four possible structures (rhombohedral, cubic, orthorhombic, and tetragonal) with ferromagnetic (FM) and with the three antiferromagnetic (AFM) orders shown schematically in Fig. 3. For the rhombohedral structure, only FM and G-type AFM spin orders were considered. The energetics is reported in Table A of SM [30]. The most stable bulk phase is rhombohedral with G-type AFM spin order and the PBE lattice parameters are in excellent agreement with experiments—see the *Bulk phase* section of SM [30] (see, also, Refs. [11–13] therein)—and with previous calculations [16].

Having demonstrated the reliability of the geometrical optimization for the bulk phases, we now focus on the multilayer system. We build the multilayers along the [001] direction and perform complete structural optimization for all the possible magnetic structures in the one-layer (1L) and two-layer (2L) cases, while for the three- and four-unit-cell flakes only the most stable spin orders have been taken into account. In the case of the cubic phase, we also study the energy difference between the ferromagnetic and antiferromagnetic state at all thicknesses. The results regarding the relative stabilities of all of the multilayers systems are reported in Table I.

The most stable phase at $T = 0\,\mathrm{K}$ in the 2D limit for freestanding $BiFeO_3$ is the orthorhombic G-type AFM, in stark contrast with bulk and supported thin films where the most stable phase is the G-type rhombohedral, while the orthorhombic structure is nonmagnetic and stable only above 820–827 K. The electronic structure of the orthorhombic G phase as a function of thickness is shown in Fig. 5, where we also include the hypothetical electronic structure of a bulk G-type AFM orthorhombic structure for comparison. In the single-layer case, the direct gap in PBE is $\approx 0.4\,\mathrm{eV}$ at the Y point. The gap increases with n, and for $n > 4$ there is a transition to an indirect gap, as can be seen by comparing with the bulk electronic structure. As it is well known that semilocal functionals tend to underestimate the gap value, we have optimized the structure and computed the electronic bands of the orthorhombic AFM G-type phase, both for the bulk and fr the ultrathin films of up to four layers by using the PBE0 functional [37]. The results are reported in Fig. 4. Even in this case all systems are insulators, as expected, but the band gap is substantially larger: E_g is 3.59 eV for the bulk, while the multilayers exhibit band gaps of 4.14, 3.96, and 3.79 eV for 1, 2, and 3 layers, respectively. Nevertheless, the gap nature is preserved: in the bulk we have an indirect band gap, while multilayers show a direct band gap for thickness below 4 layers.

The second most stable phase is the cubic ferromagnetic phase having a metallic ground state, in the case of monolayer and bilayers, while for thicker multilayers the most stable spin polarization is AFM G. However, the energy difference is very small (see Table I), making them almost degenerate. We also

TABLE I. Relative energies and magnetic moments per formula unit of $BiFeO_3$ for all possible stoichiometric $BiFeO_3$ single- and bilayers calculated with the PBE functional. The energies are given with respect to the orthorhombic AFM G structure. C = cubic, PC = pseudocubic, O = orthorhombic, and T = tetragonal.

Structure	ΔE 1L (eV)	$\langle\mu\rangle$ 1L	ΔE 2L (eV)	$\langle\mu\rangle$ 2L	ΔE 3L (eV)	$\langle\mu\rangle$ 3L	ΔE 4L (eV)	$\langle\mu\rangle$ 4L
C FM	0.386	2.57	0.447	2.51	0.411	2.74	0.511	2.64
C AFM A	–	–	0.498	2.55	–	–	–	
C AFM C	–	–	0.526	2.48	–	–	–	
C AFM G	0.469	3.28	0.489	2.90	0.359	2.76	0.485	2.90
PC Fer	0.871	3.31	0.980	2.07	–	–	–	
PC AFM A	–	–	0.988	2.20	–	–	–	
PC AFM C	–	–	0.843	2.65	0.510	2.75	0.650	2.98
PC AFM G	0.512	2.87	0.951	2.66	–	–	–	
O FM	0.088	2.70	0.171	2.79	–	–	–	
O AFM A	–	–	0.189	3.18	–	–	–	
O AFM C	–	–	0.091	3.35	–	–	–	
O AFM G	0.000	3.39	0.000	3.36	0.000	3.35	0.000	3.36
T FM	0.432	2.56	0.762	2.81	–	–	–	
T AFM A	–	–	0.705	2.57	–	–	–	
T AFM C	–	–	0.771	2.61	–	–	–	
T AFM G	0.387	3.43	0.491	2.71	0.792	2.87	0.660	2.87

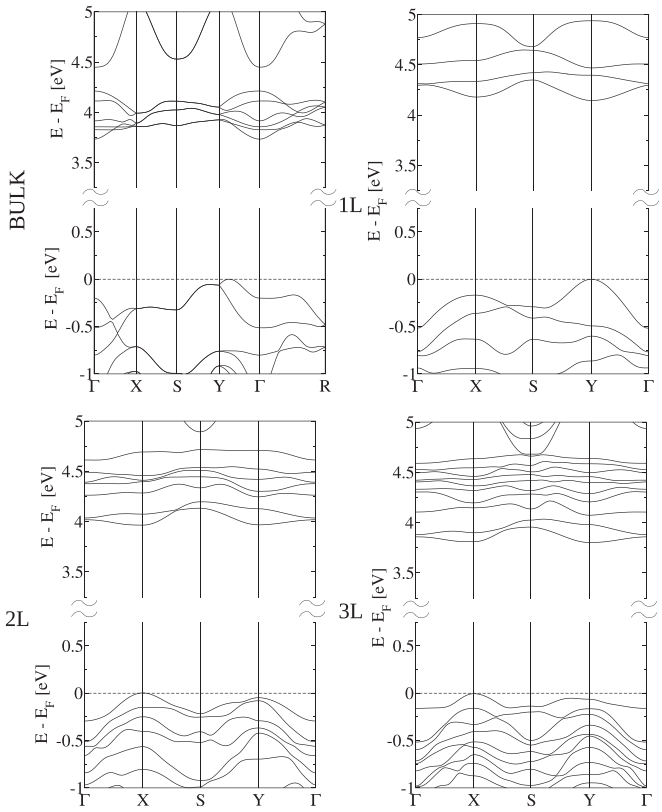

FIG. 4. Electronic structure of orthorhombic multilayers with G-type antiferromagnetic order computed at PBE0 level of theory.

stabilize another polytype that we label pseudocubic as it is a variant of the cubic phase but with a substantial distortion (see Fig. 2) and an in-plane crystallographic angle slightly different from 90°. However, its energy is substantially larger, but it becomes more stable by increasing the number of multilayers (see Fig. 2). The pseudocubic phase arises from the pseudocubic lattice formed by Bi atoms in bulk rhombohedral structure, hence it is related to the *R*3*c* phase [38].

Our findings show that the orthorhombic G phase is the most stable at low temperature. This result is very promising as it shows that the 2D limit can then be used to synthesize freestanding ultrathin perovskites with unexpected crystal properties and magnetic orders. Indeed, the orthorhombic polytype is nonmagnetic in bulk as it is only stable at very high temperatures (see Fig. 1), while it is an antiferromagnetic ferroelectric in few-layer form.

Our results disagree with a very recent experimental paper [1] detecting enhanced tetragonality in few-atom-thick flakes, as the orthorhombic G phase does not show enhanced tetragonality in the 2D limit. Furthermore structural parameters disagree with experimental data (see Fig. 6 for behavior of c/a as a function of thickness and comparison to experiments from Ref. [1]). This could stem from the fact that in experiments thick films have been grown on a $SrTiO_3$ substrate and have been prepared at low T from the rhombohedral AFM G-type structure. When the film is released from the substrate in its freestanding form, the resulting structure could be metastable and is not necessarily the most stable one. This thesis is validated by similar behaviors occurring in thicker films.

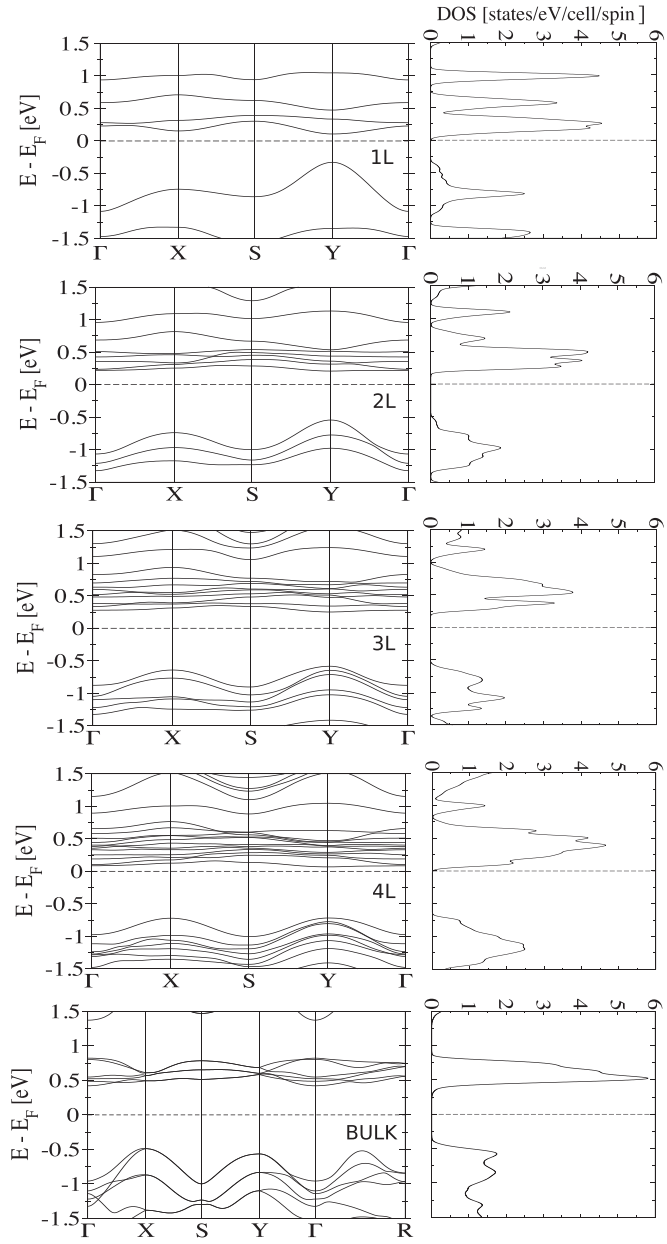

FIG. 5. Electronic structure and density of states of orthorhombic multilayers with G-type antiferromagnetic order computed at PBE level.

In an effort to clarify the possible $BiFeO_3$ polytypes detected in experiments, we consider all the most stable structures of all $BiFeO_3$ multilayers and plot in Fig. 6 the structural parameters as a function of layer thickness against experimental data from Ref. [1]. In our analysis, we define c as the distance of the Bi atoms along the z direction while a is the Bi-Bi distance along the xy plane. In the case of tetragonal and cubic structures, because of symmetry, there is only one possible value for c. In the absence of symmetries (pseudocubic case), we defined c as the averaged distance of the Bi atoms along z. Finally, we plot the distortion parameter ΔFe that is the offset long the c axis of the Fe atoms from the center of the four neighboring Bi atoms and is shown in Fig. 6.

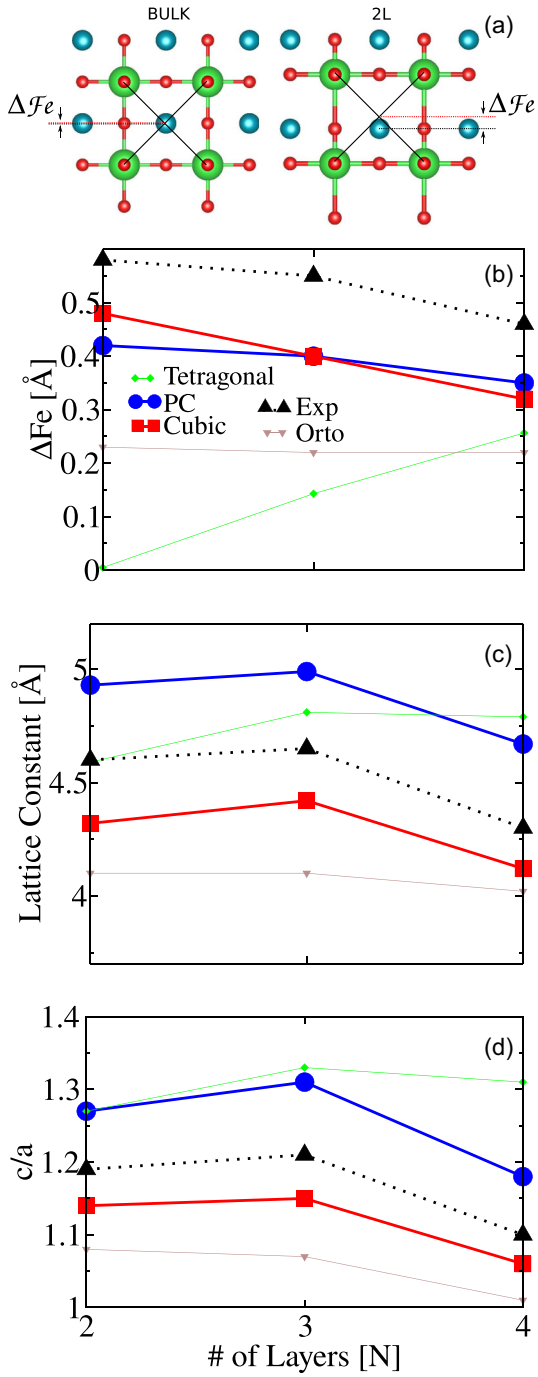

FIG. 6. (a) Structure of the four-unit cell for bulk and 2L. Off center (ΔFe) is defined as the distance along the the out-of-plane direction between the center of the neighboring Bi ions (red dotted line) and the Fe ions (black dotted line). The Bi atoms are reported in green, the O atoms in dark red, the Fe atoms in cyan. (b) Offset of the Fe atoms along z from the plane formed by the four neighboring Bi ions. (c) The lattice c. (d) c/a ratio. All of the quantities are reported as a function of the number of layers, N.

As can be seen from Fig. 6, the most stable AFM G orthorhombic phase exhibits a maximum value of c/a ratio of 1.08 and thus an insufficient tetragonal distortion. Moreover both the in-plane lattice parameter and the distortion are too small and practically independent of the number of layers, in disagreement with experimental data. This excludes the result that the freestanding films in Ref. [1] are orthorhombic. In contrast, both cubic FM and AFM G (the structural data for the former is reported in Fig. 6; for the latter see Table B of SM [30]) pseudocubic and tetragonal lattices show a T-like distortion. The latter has, as expected, the biggest c/a value of 1.33 for the trilayer case; however the behavior of c/a and of the Fe offset as a function of thickness are in stark disagreement with experiments, as shown in Figs. 6(a) and 6(c). A similar trend has been found for the cubic lattice with AFM G spin polarization. This confirms that neither the tetragonal phase nor the cubic AFM G phase are detected in experiments. In contrast, both the cubic FM and pseudocubic AFM C structures exhibit dependence of the structural parameters in agreement with experimental data, the cubic phase being the closer to the experiments. It is worth noting that the cubic structure is the second most favorite in absolute terms, even in the absence of external strain (see Table I).

Even if our results explain the experimental structural data in Ref. [1], they disagree with the claim that the most stable structure is the tetragonal one. The paucity of technical details in Ref. [1] does not allow for an explanation of the disagreement. However, we point out that starting from the structure in Fig. 4 of Ref. [1] we were unable to obtain the same results as a function of layer thickness. Reference [1] claimed that a $BiFeO_3$ multilayer has tetragonal symmetry (see Fig. 4), but in our results we found that multilayers $BiFeO_3$ with tetragonal symmetry are not able to reproduce experimental data.

Finally, we remark that the distortion in few-layer $BiFeO_3$ is present (and is practically identical) even if we artificially suppress the magnetic order (i.e., perform a spinless electron calculation). This suggests that few-layer $BiFeO_3$ is a type I multiferroic [9,10]. In Ref. [1] it is claimed that the freestanding films with enhanced tetragonality host a gigantic dipole moment per unit surface. The claim is based on out-of-plane piezoresponse force microscopy of $BiFeO_3$ thin films grown on top of $SrTiO_3$, showing the occurrence of a hysteresis loop. However, some care is needed, as also $SrTiO_3(100)$ is a polar surface (sometimes labeled *weakly polar* [39,40]) and it could contribute to the measured polarization in a non-negligible way. In order to verify the possible occurrence of a surprising "polar" metallic state, we first calculate the electronic structure of both cubic and pseudocubic phases as a function of thickness. We find that the system is metallic at all thicknesses (see Figs. S4, S5, and 7), in agreement with what happens also in the bulk case, namely a transition to a metallic state at high temperature when the cubic phase is stabilized (see Fig. 1) [20]. However, the lack of periodicity in cubic or pseudocubic multilayers and the different terminations of the top and bottom faces leads to broken inversion symmetry along the z axis. This allows for nonzero c-axis component of the forces acting on the Fe atoms. As a result the Fe atoms undergo a distortion along z. In the bulk the distortion is frozen by the symmetry, while in a very thick film it would be confined on the outer layers. In the case $n \leqslant 4$ the distortion is sizable on all the Fe atoms throughout the full flake. We have then the case of a cubic metallic phase with a distortion of Fe atoms along the z axis. It is natural to investigate if a finite dipole moment per unit surface occurs due to the distortion.

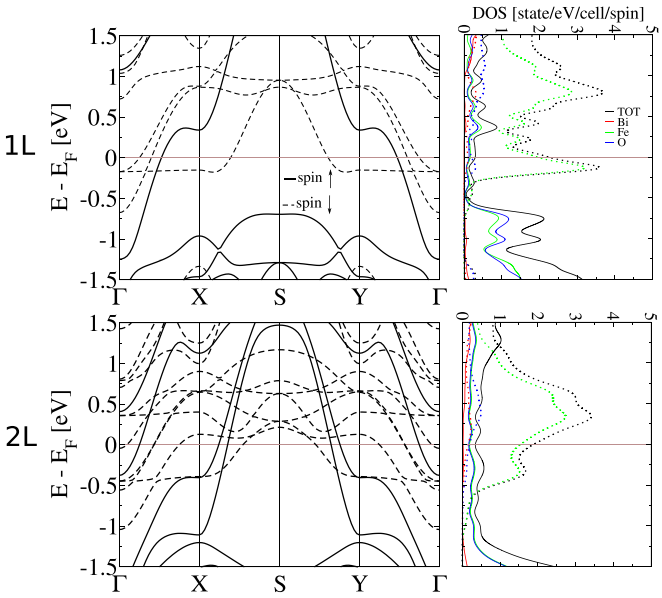

FIG. 7. Electronic structure and density of states (including their projections onto each atom) of cubic FM monolayer and bilayers systems. The solid lines refer to the majority spin channel (denoted as spin up), while the dotted lines refer to the minority spin channel (denoted as spin down).

We then compute the dipole moment in the z direction where no periodicity occurs (see SM [30] for more information). In the case of 2D material the polarization is obtained by multiplying the charge by the distance, as reported in Ref. [41], while in a 3D system this quantity is divided by the cell unit volume in order to obtain a surface density polarization. For completeness we report the volume of the layered systems beside the polarization. The dipole moment for the cubic FM metallic multilayers is approximately $P_z \approx 23 \times 10^{-3}$ (V = 14.53 Å^3) e Å/f.u. and $P_z \approx 40 \times 10^{-3}$ e Å/f.u. (V = 43.44 Å^3) for the monolayer and bilayers respectively. These values are of the same order as those found in $LiOsO_3$ multilayers [41]. For completeness, we also performed the same calculation for the pseudocubic phases, obtaining values a factor of about 10 bigger: $P_z \approx 243 \times 10^{-3}$ e Å/Bi ($V = 21.82$ Å^3) and $P_z \approx 415 \times 10^{-3}$ e Å/Bi ($V = 62.74$ Å^3). Hence, a large polarization is predicted, consistent with a recent experimental report [1].

Thus, both structural parameters and the large dipole moment per unit surface of the cubic and pseudocubic phases are in excellent agreement with experiments, with the structural parameters of the cubic phase in slightly better agreement. This demonstrates that $BiFeO_3$ multilayers are metals undergoing a distortion and hosting a finite dipole moment per unit surface, i.e., Anderson-Blount [42] metals.

IV. OUTLOOK

In this paper we studied the structural, magnetic, and electronic properties of $BiFeO_3$ multilayers with $n \leqslant 4$. These multilayers were recently synthesized in freestanding form [1–3], but little is known about their physical properties. We obtained two crucial results. The first is that in the absence of external strain the most stable polytype is orthorhombic with AFM G magnetic order. The orthorhombic phase is normally called the β phase in bulk form and is a nonmagnetic paraelectric phase stable only at high temperatures, largely above the magnetic ordering transition. Our work shows that in ultrathin films it can be stabilized in "antiferromagnetic" and "ferroelectric" forms, where the emergence of a dipole moment along the z axis is due to the stoichiometricity of the multilayers that, having different top and bottom terminations, allows for a finite force on the Fe atoms, an effect not possible in bulk form. Furthermore, these multilayers undergo a direct to indirect gap transition by increasing thickness, that could lead to remarkable optical properties. The optimization of synthesis conditions could open the perspective to investigate this yet experimentally undetected $BiFeO_3$ phase.

The second important result is that we have identified the crystal structure of the exfoliated $BiFeO_3$ flakes as being the cubic FM polytype, in contrast with previous claims [1]. It is noteworthy that even if the energy difference between the orthorhombic and cubic phases is quite sizable, we have to consider that the experimental freestanding BiFeO3 films reported in Ref. [1] have been obtained by deposition of $BiFeO_3$ on $SrTiO_3$. Probably, starting from a different substrate, it is possible to obtain $BiFeO_3$ films with different symmetry. This could make the cubic phase metastable despite the large energy difference. In these multilayers, the broken inversion symmetry with respect to the plane generates a distortion coexisting with metallicity. Moreover, the calculated dipole moment along the z axis is in agreement with the measurements from piezoresponse force microscopy. Thus, few-layer cubic $BiFeO_3$ could be a physical realization of the "polar" metallic state proposed many years ago by Anderson and Blount [42] and detected only in few materials up to now [41,43–48].

ACKNOWLEDGMENTS

We acknowledge support from the European Union's Horizon 2020 research and innovation program Graphene Flagship under Grant Agreement No. 881603. We acknowledge the CINECA award under the ISCRA initiative, for the availability of high performance computing resources and support. We acknowledge Prof. Tula Paudel for helpful conversations on the topic. M.C. acknowledges Prof. Yuefeng Nie and Prof. Zhengbin Gu for fruitful discussions.

[1] D. Ji, S. Cai, T. R. Paudel, H. Sun, C. Zhang, L. Han, Y. Wei, Y. Zang, M. Gu, Y. Zhang *et al.*, Nature (London) **570**, 87 (2019).

[2] D. Lu, D. Baek, S. Hong, L. F. Kourkoutis, Y. Hikita, and H. Y. Hwang, Nat. Mater. **15**, 1255 (2016).

[3] S. S. Hong, J. H. Yu, D. Lu, A. F. Marshall, Y. Hikita, Y. Cui, and H. Y. Hwang, Sci. Adv. **3**, eaao5173 (2017).

[4] B. Peng, R.-C. Peng, Y.-Q. Zhang, G. Dong, Z. Zhou, Y. Zhou, T. Li, Z. Liu, Z. Luo, S. Wang *et al.*, Sci. Adv. **6**, eaba5847 (2020).

[5] J. G. Bednorz and K. A. Müller, Z. Phys. B **64**, 189 (1986).
[6] A. von Hippel, R. G. Breckenridge, F. G. Chesley, and L. Tisza, Ind. Eng. Chem. **38**, 1097 (1946).
[7] N. A. Spaldin and M. Fiebig, Science **309**, 391 (2005).
[8] P. R. Paudel (private communication).
[9] D. Khomskii, Physics **2**, 20 (2009).
[10] Ravi Shankar P N, S. Mishra, and S. Athinarayanan, APL Mater. **8**, 040906 (2020).
[11] J. R. Teague, R. Gerson, and W. J. James, Solid State Commun. **8**, 1073 (1970).
[12] K. Ueda, H. Tabata, and T. Kawai, Appl. Phys. Lett. **75**, 555 (1999).
[13] V. R. Palkar, J. John, and R. Pinto, Appl. Phys. Lett. **80**, 1628 (2002).
[14] K. Y. Yun, D. Ricinschi, T. Kanashima, M. Noda, and M. Okuyama, Jpn. J. Appl. Phys. **43**, L647 (2004).
[15] K. Y. Yun, M. Noda, and M. Okuyama, Appl. Phys. Lett. **83**, 3981 (2003).
[16] P. Ravindran, R. Vidya, A. Kjekshus, H. Fjellvåg, and O. Eriksson, Phys. Rev. B **74**, 224412 (2006).
[17] D. Ricinschi, K.-Y. Yun, and M. Okuyama, J. Phys.: Condens. Matter **18**, L97 (2006).
[18] P. Fischer, M. Polomska, I. Sosnowska, and M. Szymanski, J. Phys. C: Solid State Phys. **13**, 1931 (1980).
[19] B. Ruette, S. Zvyagin, A. P. Pyatakov, A. Bush, J. F. Li, V. I. Belotelov, A. K. Zvezdin, and D. Viehland, Phys. Rev. B **69**, 064114 (2004).
[20] R. Palai, R. S. Katiyar, H. Schmid, P. Tissot, S. J. Clark, J. Robertson, S. A. T. Redfern, G. Catalan, and J. F. Scott, Phys. Rev. B **77**, 014110 (2008).
[21] I. A. Kornev, S. Lisenkov, R. Haumont, B. Dkhil, and L. Bellaiche, Phys. Rev. Lett. **99**, 227602 (2007).
[22] D. C. Arnold, K. S. Knight, G. Catalan, S. A. Redfern, J. F. Scott, P. Lightfoot, and F. D. Morrison, Adv. Funct. Mater. **20**, 2116 (2010).
[23] M. Yaakob, M. Taib, M. Deni, and M. Yahya, Integr. Ferroelectr. **155**, 134 (2014).
[24] J.-H. Lee, M.-A. Oak, H. J. Choi, J. Y. Son, and H. M. Jang, J. Mater. Chem. **22**, 1667 (2012).
[25] D. V. Karpinsky, E. A. Eliseev, F. Xue, M. V. Silibin, A. Franz, M. D. Glinchuk, I. O. Troyanchuk, S. A. Gavrilov, V. Gopalan, L.-Q. Chen *et al.*, npj Comput. Mater. **3**, 20 (2017).
[26] R. Zeches, M. Rossell, J. Zhang, A. Hatt, Q. He, C.-H. Yang, A. Kumar, C. Wang, A. Melville, C. Adamo *et al.*, Science **326**, 977 (2009).
[27] D. Mazumdar, V. Shelke, M. Iliev, S. Jesse, A. Kumar, S. V. Kalinin, A. P. Baddorf, and A. Gupta, Nano Lett. **10**, 2555 (2010).
[28] D. Lebeugle, D. Colson, A. Forget, and M. Viret, Appl. Phys. Lett. **91**, 022907 (2007).
[29] R. Haumont, I. A. Kornev, S. Lisenkov, L. Bellaiche, J. Kreisel, and B. Dkhil, Phys. Rev. B **78**, 134108 (2008).
[30] See Supplemental Material at http://link.aps.org/supplemental/10.1103/PhysRevB.104.174111 for computational details and for additional tables and figures.
[31] J. P. Perdew, K. Burke, and M. Ernzerhof, Phys. Rev. Lett. **77**, 3865 (1996).
[32] P. Giannozzi, S. Baroni, N. Bonini, M. Calandra, R. Car, C. Cavazzoni, D. Ceresoli, G. L. Chiarotti, M. Cococcioni, I. Dabo *et al.*, J. Phys.: Condens. Matter **21**, 395502 (2009).
[33] P. Giannozzi, O. Andreussi, T. Brumme, O. Bunau, M. B. Nardelli, M. Calandra, R. Car, C. Cavazzoni, D. Ceresoli, M. Cococcioni *et al.*, J. Phys.: Condens. Matter **29**, 465901 (2017).
[34] C. Adamo and V. Barone, J. Chem. Phys. **110**, 6158 (1999).
[35] R. Dovesi, R. Orlando, A. Erba, C. M. Zicovich-Wilson, B. Civalleri, S. Casassa, L. Maschio, M. Ferrabone, M. De La Pierre, P. D'Arco *et al.*, Int. J. Quantum Chem. **114**, 1287 (2014).
[36] T. Sohier, M. Calandra, and F. Mauri, Phys. Rev. B **96**, 075448 (2017).
[37] C. Franchini, J. Phys.: Condens. Matter **26**, 253202 (2014).
[38] J. B. Neaton, C. Ederer, U. V. Waghmare, N. A. Spaldin, and K. M. Rabe, Phys. Rev. B **71**, 014113 (2005).
[39] J. Goniakowski and C. Noguera, Surf. Sci. **365**, L657 (1996).
[40] C. Noguera and J. Goniakowski, Chem. Rev. **113**, 4073 (2013).
[41] J. Lu, G. Chen, W. Luo, J. Íñiguez, L. Bellaiche, and H. Xiang, Phys. Rev. Lett. **122**, 227601 (2019).
[42] P. W. Anderson and E. I. Blount, Phys. Rev. Lett. **14**, 217 (1965).
[43] Y. Shi, Y. Guo, X. Wang, A. J. Princep, D. Khalyavin, P. Manuel, Y. Michiue, A. Sato, K. Tsuda, S. Yu *et al.*, Nat. Mater. **12**, 1024 (2013).
[44] T. H. Kim, D. Puggioni, Y. Yuan, L. Xie, H. Zhou, N. Campbell, P. J. Ryan, Y. Choi, J. W. Kim, J. R. Patzner *et al.*, Nature (London) **533**, 68 (2019).
[45] N. J. Laurita, A. Ron, J. Y. Shan, D. Puggioni, N. Z. Koocher, K. Yamaura, Y. Shi, J. M. Rondinelli, and D. Hsieh, Nat. Commun. **10**, 3217 (2019).
[46] J. Wang, L. Yang, C. W. Rischau, X. Zhuokai, Z. Ren, T. Lorenz, J. Hemberger, X. Lin, and K. Behnia, npj Quantum Mater. **4**, 61 (2019).
[47] A. Filippetti, V. Fiorentini, F. Ricci, P. Delugas, and J. Íñiguez, Nat. Commun. **7**, 11211 (2016).
[48] A. Urru, F. Ricci, A. Filippetti, J. Íñiguez, and V. Fiorentini, Nat. Commun. **11**, 4922 (2020).